J Appl Electrochem (2008) 38:259–268
DOI 10.1007/s10800-007-9435-9

ORIGINAL PAPER

Electrochemical deposition of platinum nanoparticles on different carbon supports and conducting polymers

Sonia Domínguez-Domínguez · Joaquín Arias-Pardilla · Ángel Berenguer-Murcia · Emilia Morallón · Diego Cazorla-Amorós

Received: 3 July 2007 / Revised: 3 October 2007 / Accepted: 16 October 2007 / Published online: 6 November 2007

Abstract Electrodeposition of Pt nanoparticles under potentiostatic conditions was performed on several types of carbon electrode supports: commercial macroporous carbon (a three-dimensional electrode), glassy carbon and graphite. Conducting polymers (poly-aniline and poly-*o*-aminophenol) were also used. The platinum nanoparticles were obtained by different Potential Step Deposition (PSD) methods in 5 mM H_2PtCl_6 + 0.5 M H_2SO_4 aqueous solutions. The effect of the final potential, time and number of steps on the quantity, distribution and size of the platinum nanoparticles was analysed. The mechanism of the electrochemical deposition of platinum was studied through the application of theoretical modelling. The progressive nucleation mechanism provided the closest agreement with the results obtained. In addition, the chemical state and morphology of the electrodeposited materials were determined by means of SEM, TEM and XPS. The results show that the carbon material structure has a strong influence on the Pt particle structure and this, in turn, affects the catalytic activity.

Keywords Carbon supports · Conducting polymers · Electrodeposition · Platinum · Electrocatalysis.

S. Domínguez-Domínguez · Á. Berenguer-Murcia · D. Cazorla-Amorós
Dpto. Química Inorgánica and Instituto Universitario de Materiales, Facultad de Ciencias, Universidad de Alicante, Ap. 99, Alicante 03080, Spain

J. Arias-Pardilla · E. Morallón (✉)
Dpto. Química Física and Instituto Universitario de Materiales, Universidad de Alicante, Ap. 99, Alicante 03080, Spain
e-mail: morallon@ua.es

1 Introduction

Several procedures have been employed to prepare Pt-supported nanoparticles on different supports, including wet impregnation [1, 2], microwave irradiation [3], microemulsion [4, 5], polyol process [6, 7], microwave assisted polyol process [8] or two-step spray pyrolysis [9]. On the other hand, electrochemical deposition is an efficient method for the preparation of metal particles. It is widely used with different strategies/methodologies, such as cyclic voltammetry [10, 11], potential step deposition [12–15] and double-pulse [16–18]. Among these, potential step deposition (PSD) provides a tool to fine-tune the amount of metal deposited, the number of metallic sites and their size.

Carbon materials are of special interest due to their outstanding properties, such as their tuneable shape, size and porosity, chemical stability, corrosion resistance, low cost, good thermal resistance and electrical conductivity [19–21]. The combination of all these characteristics has promoted the use of these materials as electrode supports. Previous work carried out in Alicante has resulted in the deposition of noble metals, by electrochemical methods, onto different carbon supports [22–24].

Conducting polymers are useful supports for the immobilisation of dispersed noble metal catalysts, due to the prevention of particle agglomeration. The porous structure and high surface area of many conducting polymers have led to their use as supporting materials in the development of new electrocatalytic materials. Due to the relative high electric conductivity of some polymers it is possible to transfer electrons through polymer chains, between the electrode and dispersed metal particles, where the electrocatalytic reaction occurs [25, 26].

In this work, the influence of the different experimental variables during the Pt electrochemical deposition

(achieved by potential step methods) on the different supports, was analysed. The supports used throughout were carbon materials and conducting polymers. The carbon materials employed were graphite (both in the form of a rod and as a macroporous disc) and glassy carbon, which have very important differences from a structural point of view. The use of such different materials affords information on the effect of the electrode support structure on the Pt deposition and activity. The effect of the presence of a thin layer of conducting polymers was also analysed. The amount of deposited particles and their size was controlled by selection of the potential step deposition conditions. The outcome was an electrode homogeneously covered with metallic nuclei of a nanometer scale size and showing good dispersion. The prepared composites have been tested for the electro-oxidation of methanol.

2 Experimental

2.1 Preparation of the supports

Different carbon materials were used to prepare the working electrodes for the platinum electrodeposition: macroporous carbon disc, glassy carbon and graphite. The macroporous carbon discs were made by the agglomeration of graphite particles. The discs were cut from a macroporous carbon sheet (thickness = 0.3 mm, mean pore size 0.7 μm, exposed geometric area 2.91 cm^2) provided by Poco Graphite (DFP-1) and washed in an ultrasonic bath (with distilled water, at room temperature, for 30 min). The graphite (Ellor + 35) and glassy carbon (CV25) rods (0.3 cm in diameter) were supplied by Carbone Lorraine.

In all cases, the materials were first treated with sandpaper, before being polished with two different diamond suspensions (particle sizes 1 and 0.25 μm, respectively) and finally washed in an ultrasonic bath (with ultrapure water, for 5 min).

The conducting polymer layers were electrochemically deposited on glassy carbon by cyclic voltammetry (between 0.06 and 1.10 V, from a 0.1 M aniline or *o*-aminophenol solution, in a supporting electrolyte of 0.5 M H_2SO_4 at a scan rate of 50 mV s^{-1}). An EQCM experiment was used to calculate film thickness from polymer peak voltammetric charge [27].

2.2 Platinum electrodeposition

All experiments described in this section were performed at room temperature unless stated otherwise. The electrodeposition of platinum particles onto the different electrodes was performed in a conventional electrochemical cell, consisting of three electrodes held at room temperature. All the reagents used were of analytical grade and were used without further purification. An EG&G potentiostat/galvanostat model 263A, controlled by the program *POWER SUITE*, was employed so that the values of current and time were monitored by computer. For all the experiments the counter-electrode was a platinum wire. The reference electrode was a reversible hydrogen electrode (RHE), immersed in a 0.5 M H_2SO_4 solution, which was connected to the working electrode compartment by a Luggin capillary.

All solutions were prepared with high-purity water (resistivity $\geq$ 18 MΩ cm), which was obtained from an Elga Labwater Purelab Ultra system. The solutions used were 0.5 M H_2SO_4 (Merck, suprapur), 5 mM H_2PtCl_6 (starting material $H_2PtCl_6.6H_2O$, Sigma-Aldrich) + 0.5 M H_2SO_4 and a 0.1 M CH_3OH (Merck) + 0.5 M H_2SO_4 solution. All solutions were saturated with nitrogen before their use and this inert atmosphere was maintained during the experiments.

The platinum particles were electrochemically deposited from a 5 mM H_2PtCl_6 + 0.5 M H_2SO_4 solution under potentiostatic conditions. Thus, in order to study the influence of different parameters on the electrodeposition of platinum, four different experimental procedures were used:

Procedure (1): one step from an initial potential (0.80 V, where no deposition of platinum occurs) to different final potentials (0.20, 0.15, 0.10, and 0.05 V in which the platinum is deposited) for different times (from 0.1 to 60 s).

Procedure (2): several consecutive steps from an initial potential (0.80 V) to a final potential (0.15 V) for different times, being the total time the same as in procedure (1).

Procedure (3): one step from an initial potential (0.80 V) to an intermediate potential (−0.35, −0.25, −0.15, and 0.0 V) for 1 s, and immediately to several final potentials (0.20, 0.15, 0.10, and 0.05 V) during 6 s.

Procedure (4): multiple, consecutive steps of short time (5 ms) from an initial potential (0.80 V) to a final potential (0.00 or −0.15 V) for 5 ms and being the total time 5 s.

All runs were repeated three times in order to ensure reproducibility of the results.

The electrochemical properties of the prepared Pt-supported electrodes were tested for methanol oxidation, which was measured in a 0.1 M CH_3OH + 0.5 M H_2SO_4 solution by cyclic voltammetry, over a potential range of 0.06–1.0 V with a scan rate of 10 mV s^{-1}.

2.3 Characterisation of the Pt-supported electrodes

X-Ray Photoelectron spectra (XPS) were recorded, using a VG-Microtech Multilab electron spectrometer, in order to

investigate the oxidation state of the electrochemically deposited platinum. The prepared Pt/C electrodes were not reduced in any way before the XPS analysis, although they were exposed to air after their synthesis. The source employed was MgKα ($h\nu$ = 1253.6 eV, 1 eV = 1.603×10^{-19} J) radiation (generated from twin anodes in the constant analyser energy mode) and the pressure of the analysis chamber was maintained below 5×10^{-10} mbar. The binding energy was adjusted by setting the C 1s transition at 284.6 eV with ±0.2 eV accuracy. The intensities of the peaks were estimated by determining the integral of each peak, after subtraction of an S-shaped background and fitting of the experimental peak to Lorentzian/Gaussian lines (70%L/30%G).

The active surface area of electrodeposited Pt was measured by comparing the charge corresponding to the adsorption/desorption processes at Pt sites between 0.05 and 0.45 V of the cyclic voltammograms (CVs) of the synthesised electrodes in 0.5 M H_2SO_4 aqueous solutions, before and after platinum deposition.

The morphological characterisation of the surface of the platinum/carbon electrodes was achieved by Scanning Electron Microscopy (SEM), using JEOL JSM-840 equipment.

Transmission Electron Microscopy (TEM), using a JEOL JEM-2010 (operating at 200 kV with a structural spatial resolution of 0.5 nm), was used to observe the size of the smallest platinum particles that could not be detected with SEM images. Small quantities of sample in powder form were collected and dispersed in ethanol, then the suspension was put onto a 3-mm-diameter copper grid covered with carbon film. Finally the solvent was evaporated in air, prior to analysis by TEM.

3 Results and discussion

3.1 Preparation of Pt-supported electrodes

Figure 1a shows the results obtained by the chronoamperometric studies of three platinum deposition experiments (prepared by Procedure 1, which is outlined in Section 2.2) using a macroporous carbon disc. The current versus time transients observed are common responses for electrochemical depositions [28]. Three different zones are distinguishable, corresponding to the stages reported by Montilla et al. in the deposition of platinum on synthetic, boron-doped diamond surfaces [24]. The first zone represents the double-layer charging current and the initiation of the nucleation process. In the second zone, the current increases due to both the growth of independent nuclei and an increase in the total number of nuclei. At this point, the observed current is simply the deposition current, without any overlapping effects. In the third zone, there are two opposite effects: growth of independent nuclei and overlap, reaching a maximum of the current and then a decrease in current.

In Fig. 1a, it is shown that the electrical charge, built up in the deposition process, decreases with increase in applied potential.

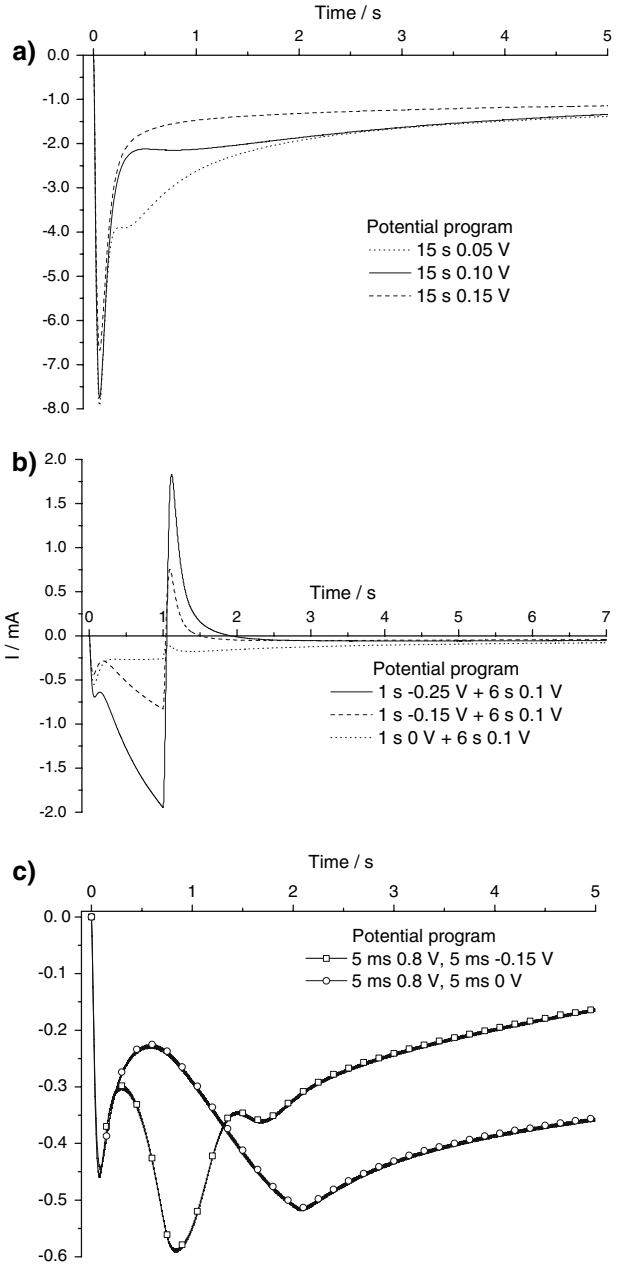

Fig. 1 Current versus time transient plot obtained during: (**a**) Potential Step Deposition of a single step (Procedure 1) with samples of macroporous carbon changing the final potential; (**b**) Potential Step Deposition of a double step (Procedure 3) with samples of glassy carbon changing the first potential and (**c**) a Potential Step Deposition of multiple steps (Procedure 4) with samples of glassy carbon changing the final potential of the steps

Table 1 shows the amount of platinum deposited during two methods, run according to Procedures 1 and 2 (which are outlined in Section 2.2). The mass of Pt deposited in each case was obtained by graphical integration of the electrical charge consumed during the deposition process Q_{Pt} (C cm^{-2}). It was assumed that the current efficiency was 100% and the following effects were negligible: partial reductions of Pt^{4+}, hydrogen evolution at the electrodeposited Pt and double layer charging. It was also assumed that the only contributing reaction was the Faradaic process (1):

$$PtCl_6^{2-} + 4e^- \rightarrow Pt + 6Cl^- \quad (1)$$

So, the quantity of deposited Pt (m_{Pt}) is obtained from Eq. 2:

$$m_{Pt} = \frac{Q_{Pt} \cdot M}{4F} \quad (2)$$

where M is the atomic weight of Pt (195.09 g mol^{-1}), and F is the Faraday constant (96485.309 C mol^{-1}).

It can be observed from Table 1 that the amount of platinum deposited, during Procedure 1, increases as a function of increasing step time. A similar trend is also observed with the application of Procedure 2. The difference in procedures is the replacement of a single, large step for several short steps (with the same final duration), without changing the initial or final potential. This trend is related to the type of particle growth and is further explained.

Figure 1b shows the chronoamperometric curves for a Potential Step Deposition experiment, according to Procedure 3. This consists of a double step process (with deposition on samples of glassy carbon) using different intermediate potentials but arriving at the same final potential. During the first step, both the deposition of platinum and the evolution of hydrogen occur simultaneously, thus producing a negative current. It can be observed that the application of a negative potential in the first step increases the amount of electrodeposited platinum (Table 2) but the charge built up, during the evolution of hydrogen, is also higher. The net result is an imprecision in the determination of the amount of platinum deposited.

The chronoamperometric curves in Fig. 1c correspond to the multiple steps of a Potential Step Deposition (carried out according to Procedure 4) on samples of glassy carbon. These curves have a very similar shape to those of the single step process (Procedure 1), any differences can be attributed to the continuous change in potential incurred by the procedure. A secondary nucleation process is thought to be responsible for the trend at times higher than 1.5 s in the graph.

From the chronoamperograms, it is possible to obtain information on the mechanism through which both nucleation and growth processes occur. Other authors [29, 30] have established mathematical current-time relationships for determining both the kinetics of the nucleation mechanism and the geometry of the growing particles. Regarding nucleation, there are two current theories. The first is that of instantaneous nucleation, in which there are a small number of active sites where the nuclei are created (at the same time) and have a slow growth. The second is progressive nucleation, in which there are many active sites. In this case, the nuclei have a fast growth rate and new nuclei are continuously formed during the deposition process. In the case of progressive nucleation, the geometry of the growing particles is estimated from the assumption that either two-dimensional (2D) islands or three-dimensional (3D) clusters are formed.

The models for the different types of nucleation and growth mechanisms are given by the following equations: (3) 2D instantaneous, (4) 2D progressive, (5) 3D instantaneous and (6) 3D progressive:

$$\frac{I}{I_m} = \frac{t}{t_m} \exp\left[-\frac{1}{2}\left(\frac{t^2 - t_m^2}{t_m^2}\right)\right] \quad (3)$$

$$\frac{I}{I_m} = \left(\frac{t}{t_m}\right)^2 \exp\left[-\frac{2}{3}\left(\frac{t^3 - t_m^3}{t_m^3}\right)\right] \quad (4)$$

$$\left(\frac{I}{I_m}\right)^2 = \frac{3.8181}{t/t_m}\left\{1 - \exp\left[-1.2564\left(\frac{t}{t_m}\right)\right]\right\}^2 \quad (5)$$

Table 1 Amount of platinum deposited on macroporous carbon by PSD from an initial potential of 0.80 V to a final potential of 0.15 V under different conditions (assuming 100% current efficiency for Pt deposition and referred to the geometric area of the carbon disc), particle size and catalytic activity towards methanol oxidation

PSD method	Number of steps	Time of steps (s)	m_{Pt} (μg cm^{-2})	S_{Pt} (m^2 g^{-1})	Particle size (nm)	Catalytic activity (A g_{Pt}^{-1})
Procedure 1	1	5	1.8	12.7	22	8
Procedure 1	1	15	2.9	12.2	23	6
Procedure 2	5	1	3.3	10.5	27	14
Procedure 2	3	5	8.2	12.8	21	6

Table 2 Amount of platinum deposited, platinum surface area, particle size and catalytic activity towards methanol oxidation obtained for Pt/macroporous carbon electrodes prepared in different PSD conditions. In all the cases the initial potential was 0.8 V

PSD Method	Conditions	m_{Pt} (μg cm^{-2})	S_{Pt} (m^2 g^{-1})	Particle size (nm)	Catalytic activity (A g_{Pt}^{-1})
Procedure 1	10 s 0 V	11.4	10.5	27	25
Procedure 1	10 s 0.05 V	9.9	21.7	13	55
Procedure 1	10 s 0.10 V	7.3	23.9	12	44
Procedure 1	10 s 0.20 V	4.7	9.5	29	12
Procedure 1	6 s 0.10 V	2.7	11.0	25	13
Procedure 3	1 s −0.35 V/6 s 0.10 V	11.5	17.9	16	41
Procedure 3	1 s -0.25 V/6 s 0.10 V	9.4	19.4	14	39
Procedure 3	1 s −0.15 V/6 s 0.10 V	5.7	21.4	13	64
Procedure 3	1 s 0 V/6 s 0.10 V	5.4	19.3	14	46
Procedure 4	−0.15 V/0.80 V 5 ms (5 s)	3.7	29.7	9	87
Procedure 4	0 V/0.80 V 5 ms (5 s)	2.7	20.4	14	40

$$\left(\frac{I}{I_m}\right)^2 = \frac{1.2254}{t/t_m}\left\{1 - \exp\left[-2.3367\left(\frac{t}{t_m}\right)^2\right]\right\}^2 \quad (6)$$

where I_m and t_m are the maximum current and time values, respectively.

With the aim of characterizing the electrodeposition process, the experimental values for platinum electrodeposits on the macroporous carbon were analysed. The current/time relationship corresponding to a Potential Step Deposition process (carried out by Procedure 1) is shown in Fig. 2, together with theoretical curves (calculated for the two types of nucleation and growth mechanisms). It is observed that the experimental curve fits best to the 3D progressive nucleation mechanism. Thus, it is assumed that the deposited particles are spherical in nature and are distributed throughout the entire electrode surface, with a rather broad particle size distribution. Even though only one example is shown, the same conclusion can also be drawn for both the graphite and glassy carbon samples. These results are in agreement with previous work carried out on the electrochemical deposition of platinum on other electrodes [24, 31]. The type of nucleation process, occurring during the electrodeposition, could be controlled by the concentration of metal precursor. This phenomenon has been observed by other authors during the deposition of platinum onto graphite [31]. The major difference between our work and that carried out by others is that in our case the concentration of 5 mM H_2PtCl_6 was kept constant in all the experiments.

In the case of Pt deposition on conducting polymers, the chronoamperometric curves obtained are very similar. However, no Pt deposition was observed using Procedure 4. Figure 3 shows the comparison between experimental data and theoretical nucleation models (3D-progressive or instantaneous). The data fit best with a 3D progressive

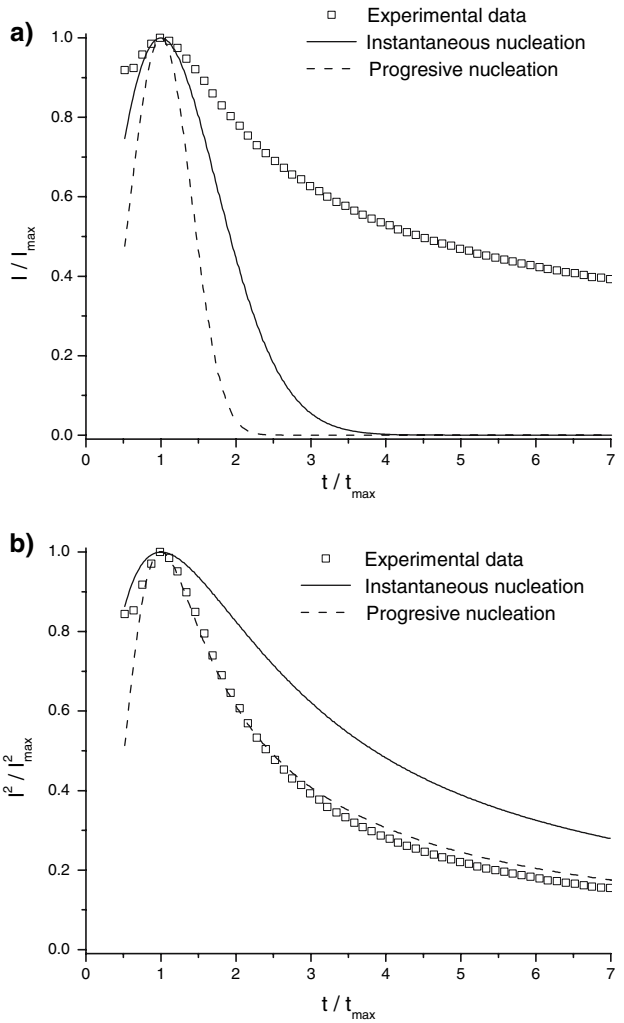

Fig. 2 Plots of the experimental data and the theoretical models of the platinum deposition on a sample of a macroporous carbon under the following conditions of Potential Step Deposition: one step from an initial potential of 0.80 V to a final potential of 0.05 V during 15 s, corresponding to (**a**) 2D and (**b**) 3D models

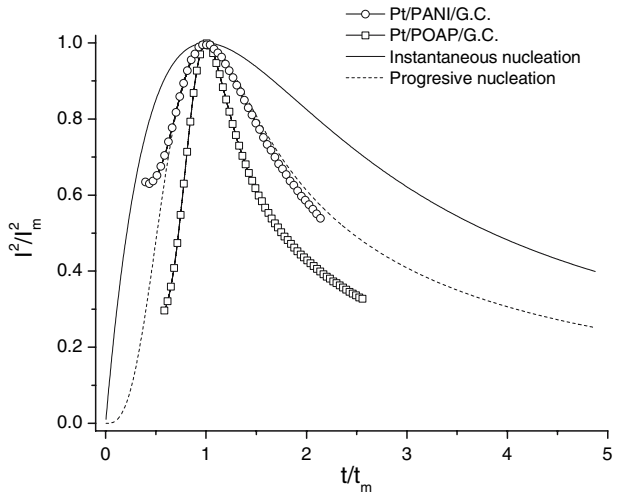

Fig. 3 Plots of the experimental data and the theoretical models for 3D nucleation of the platinum deposition on (○) PANI and (□) POAP under the following conditions of Potential Step Deposition: one step from an initial potential of 0.80 V to a final potential of 0.05 V during 60 s and thickness of polymer film 400 nm

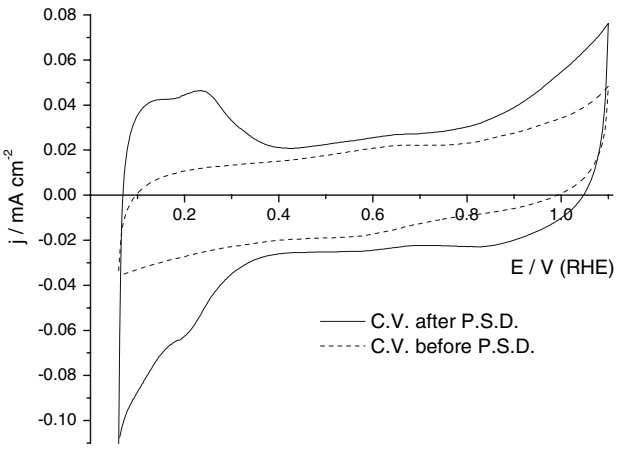

Fig. 4 The cyclic voltammograms of Pt/glassy carbon electrodes at 50 mV s^{-1}, in 0.5 M H_2SO_4 aqueous solution, before and after a Potential Step Deposition

nucleation model, for the case of Pt deposition over a PANI film (400 nm) but not for a POAP film. Similar behaviour was previously observed in Ag deposition over POAP modified electrodes [32], where a high overpotential was used for the deposition. It may be concluded that both deposition and growth mechanisms are dependant on the type of polymers employed during the deposition process.

3.2 Characterisation of Pt-supported electrodes

The chemical oxidation states of the electrodeposited Pt were determined by XPS (Figure not shown). The Pt 4f line consists of two overlapping peaks at binding energy values of about 71.1 and 74.3 eV. These values correspond to Pt $4f_{7/2}$ and Pt $4f_{5/2}$ peaks, respectively, being very close to the binding energies expected from metallic Pt. It must be noted that Pt^{2+} and Pt^{4+} would exhibit much higher binding energies [33]. These results demonstrate that platinum is essentially deposited in its metallic state during our experiments.

The active surface area(S_{Pt}: m^2 g^{-1}) of the Pt-supported electrodes can be evaluated from the electrical charge measured in the characteristic adsorption–desorption processes on Pt. The cyclic voltammogram employed is that obtained with a 0.5 M H_2SO_4 solution. Figure 4 shows the results of the cyclic voltammetry studies carried out on the glassy carbon, before and after the platinum deposition. The electrochemically active surface area is estimated with the assumption that 1 cm^2 of smooth Pt requires 210 μC [34] for the adsorption of one electron per Pt site.

The mean diameter (d, nm) of the Pt particles is calculated from the specific surface area, assuming that this value is the ratio between the area and the weight of one particle. Spherical particle geometry is also assumed and the resulting equation is (7):

$$d = \frac{6000}{\rho_{Pt} \times S_{Pt}} \tag{7}$$

where ρ_{Pt} is the platinum specific density (21.4 g cm^{-3}).

Table 2 summarises the characteristics of different platinum electrodeposits on the macroporous carbon. The platinum particle diameter (for all Procedures) varies between 9 and 30 nm. Similar results were obtained for the glassy carbon and the graphite electrodes; however, they are not shown in the table. It may be concluded that the particle size is dependent on time, the number of steps (in each Procedure) and the potentials used in each Potential Step Deposition process. It can be noted that experiments which apply an intermediate pulse, at negative potential (Procedures 3 or 4), produce smaller Pt particles yet deposit the same amount of platinum. These methods are based on two main pulses; first, a short pulse at negative potentials (where the nucleation initiates) and, second, a longer pulse at positive potentials (where the nuclei grow). During the second pulse, the potential must be positive enough to inhibit the formation of new nuclei. This allows the generation of more platinum nuclei with a controlled size distribution.

In order to verify the particle size of the deposited platinum, SEM analyses was carried out for all the Pt/C electrodes, which were prepared by Procedure 3. SEM micrographs of platinum, deposited on the three carbon supports, are shown in Fig. 5. In general, the particles exhibit uniform size and spherical shape. They appear to be homogeneously distributed over the entire support surface. In the case shown in Fig. 5 (platinum deposit prepared by

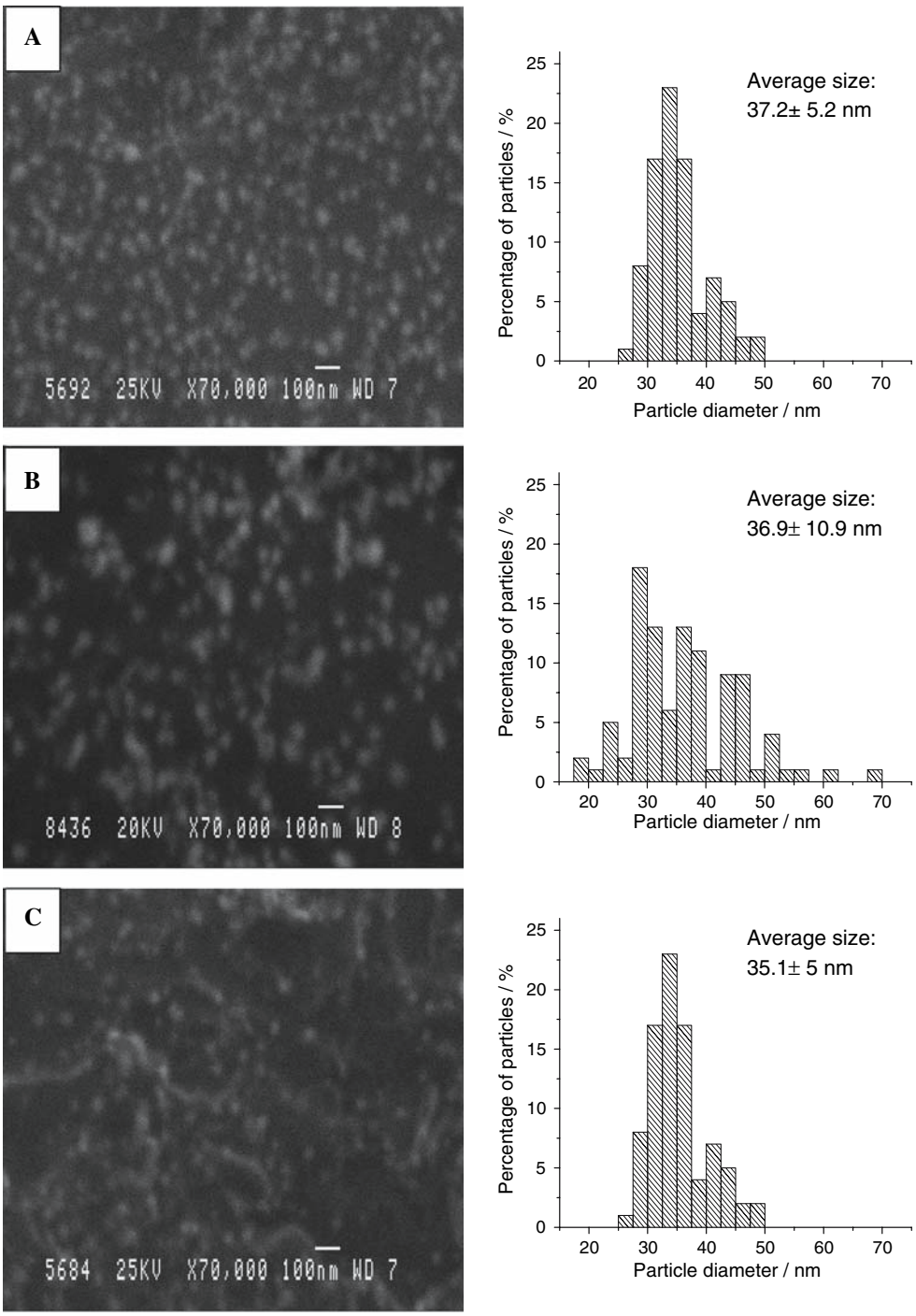

Fig. 5 SEM micrographs and their respective histogram in its right (corresponding to the particle size distributions based on a 100-particle count) of Pt deposited by PSD according to procedure 3 (from 0.80 V to an intermediate potential of − 0.15 V (1 s) and immediately to 0.10 V for 6 s) on (**a**) glassy carbon, on (**b**) macroporous carbon and on (**c**) graphite

Procedure 3), the particles are approximately 36 nm in diameter for all different types of carbon electrode.

The platinum particle size, as seen in SEM images, is rather bigger than that which was calculated *via* cyclic voltammetry. This may be due to either the impossibility of observing small particles by SEM or because the observed particles are, in fact, aggregations of smaller particles. In order to overcome these problems, TEM observations were made with the Pt/macroporous carbon (obtained according to procedure 3) as a means of characterisation. Figure 6 shows that the electrodeposited platinum particles are of different size and display diameters as small as 3–5 nm (see inset in the images). Interestingly, the particles of about 40 nm diameter comprise agglomerates of small particles of about 3–5 nm diameter (as shown in the lower image of Fig. 6). The particle sizes observed by these TEM studies are in agreement with those predicted by the cyclic voltammetry performed.

The same behaviour was observed in the Pt/conducting polymer electrodes, the platinum particle size observed in SEM images being bigger than the calculated diameter predicted by cyclic voltammetry. The obtained values (16–18 nm) are slightly bigger than those obtained (13–14 nm) without polymer film and very similar using both PANI and POAP (Table 3).

3.3 Electrocatalytic test of Pt-supported electrodes in the electro-oxidation of methanol

A series of cyclic voltammetry tests were carried out on Pt/carbon electrodes immersed in a 0.1 M CH_3OH + 0.5 M H_2SO_4 solution in order to monitor the behaviour of these electrodes towards the oxidation of methanol. The cyclic voltammograms obtained during the third cycle are displayed in Fig. 7. The oxidation peaks of methanol are observed at 0.83 and 0.79 V. The starting potential of methanol oxidation was observed as 0.49 V for the glassy carbon electrode and 0.55 V for both the macroporous carbon and graphite electrodes. Similar values were obtained when conducting polymers were used as supports. The catalytic activity of a catalyst is defined as the maximum current obtained during the third cycle of the methanol oxidation, per weight of Pt.

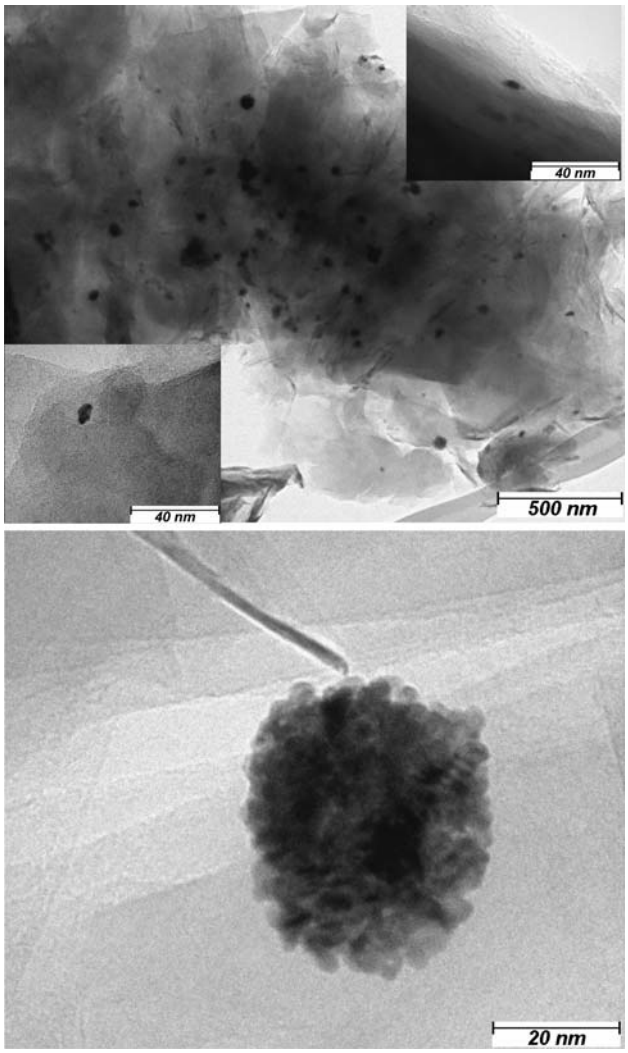

Fig. 6 TEM images of Pt deposited by PSD according to procedure 3 (from 0.80 V to an intermediate potential of −0.25 V for 1 s, and immediately to 0.10 V for 6 s) on the macroporous carbon

Tables 1 and 2 show the values of catalytic activity towards methanol oxidation, for all procedures, using Pt/macroporous carbon electrode. Similar behaviour was observed with graphite and glassy carbon samples. It can be observed that a multiple step deposition procedure produces the best catalytic activity towards methanol oxidation. The improvement in catalytic activity due to the use of a Multiple Step Deposition method, compared to the other three procedures, has been observed in other work [35].

The best conditions for deposition onto each electrode were determined with respect to the following experimental parameters; potential applied during each step, time of each step. The electrocatalytic activity of the resulting Pt/C deposit was also considered. Table 4 compares both the catalytic activity of the catalysts prepared (with the different supports) and the optimal experimental conditions for each sample.

The catalytic activity obtained with the Pt/macroporous carbon electrode is about 1.7 times higher than the other electrodes. The improved performance of the macroporous carbon support is a result of its characteristic porosity, which allows for a better particle distribution over the support and leads to smaller particles sizes. The characteristic porosity of macroporous carbon means that the entire 3D surface can be considered a functioning electrode. The catalytic activities for these Pt/carbon electrodes (summarised in Table 4) are higher than, or similar to, those previously reported [16, 24, 36]. In the case of Pt/conducting polymer the activity values are lower, but there is no significant difference between PANI and POAP. With the experimental conditions used, the introduction of a thin polymer film onto the electrode does not increase the catalytic activity.

A plot of the catalytic activity versus particle size (of the platinum-supported electrodes, obtained by the all four procedures) can be seen in Fig. 8. The activity of a Pt/Vulcan catalyst is included, for comparative purposes [37]. The activity of the Pt/Vulcan sample has been corrected to take into account the different scan rates used in the cyclic voltammetry experiments. (50 mV s^{-1} for Pt/Vulcan and 10 mV s^{-1} in this work). The catalytic activity obtained by the electrodeposition method is of the same order of magnitude as that obtained for the Pt/Vulcan sample, which

Table 3 Amount of platinum deposited, platinum surface area, particle size and catalytic activity towards methanol oxidation obtained for Pt/polymer/Glassy carbon electrodes prepared in different PSD conditions. In all the cases the initial potential was 0.80 V and thickness of polymer film 130 nm

Composite	PSD method	Conditions	m_{Pt} (μg cm^{-2})	S_{Pt} (m^2 g^{-1})	Particle size (nm)	Catalytic activity (A g_{Pt}^{-1})
PANI/G.C.	Proc. 1	30 s 0.10 V	19.6	16.3	17	30
PANI/G.C.	Proc. 3	1 s −0.25 V/30 s 0.1 V	18.6	17.1	16	31
PANI/G.C.	Proc. 3	1 s −0.15 V/30 s 0.1 V	12.6	17.3	16	30
PANI/G.C.	Proc. 3	1 s −0.25 V/6 s 0.1 V	3.6	16.1	17	29
PANI/G.C.	Proc. 3	1 s −0.15 V/6 s 0.1 V	3.7	17.7	16	30
POAP/G.C.	Proc. 1	30 s 0.05 V	9.7	16.1	17	24
POAP/G.C.	Proc. 3	1 s −0.25 V/30 s 0.1 V	23.8	14.9	19	35
POAP/G.C.	Proc. 3	1 s −0.15 V/30 s 0.1 V	23.5	14.7	19	36
POAP/G.C.	Proc. 3	1 s −0.25 V/6 s 0.1 V	3.3	15.3	18	19

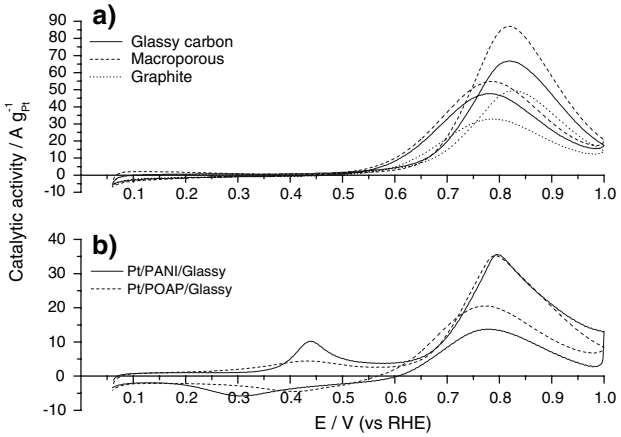

Fig. 7 Cyclic voltammograms of the third cycle for the best Pt/carbon and Pt/conducting polymer electrodes obtained at 10 mV s^{-1}, in 0.1 M MeOH + 0.5 M H_2SO_4 solution

was prepared by a chemical method. The catalytic activity towards methanol oxidation increases as the platinum particle size decreases, reaching a maximum (at around 9 nm). This suggests that the optimal platinum particle size is between 2 and 10 nm, a conclusion that has been drawn by other authors [38, 39]. Particles with smaller or bigger diameters show less activity for methanol oxidation [38, 39]. In the case of Pt/glassy carbon electrodes an increased catalytic activity is observed for a platinum particle size of around 20 nm. This suggests that the platinum particle structure is significantly different in the case of the glassy carbon support. Both the graphite rod and the macroporous carbon show similar structures, which is unsurprising since the macroporous carbon is prepared by graphite particle agglomeration. Both of these supports are structurally different to the glassy carbon support. The surface crystallinity of the support is thought to have a significant influence on the materials behaviour. The presence of a larger number of defects in the glassy carbon electrode, in comparison to the graphite electrode, may account for the existence of preferential nucleation sites (which would lead to a better dispersion of platinum particles). Deposition of the polymer film onto the glassy carbon support eliminates these structural differences. This, in turn, confirms the relevance of the glassy carbon structure towards the platinum particle structure.

4 Conclusions

Highly dispersed platinum particles were electrodeposited, via potential step deposition methods onto the following supports: macroporous carbon, glassy carbon, graphite and conducting polymers (polyaniline and poly-*o*-aminophenol).

Table 4 Amount of platinum deposited, platinum surface area, particle size and catalytic activity towards methanol oxidation for the three Pt/carbon electrodes prepared by different methods 0.1 M MeOH + 0.5 M H_2SO_4 aqueous solution with a scan rate of 10 mV s^{-1}

PSD method	Conditions	m_{Pt} (μg cm^{-2})	S_{Pt} (m^{2}g^{-1})	Particle size (nm)	Catalytic activity (A g_{Pt}^{-1})
Macroporous Disc (Proc. 4)	0.80 V/0.15 V 5 ms (5s)	3.7	29.7	9	87
Glassy carbon (Proc. 4)	0.80 V/0.15 V 5 ms (5s)	10.6	12.6	22	56
Glassy carbon (Proc. 3)	1 s −0.15 V/6 s 0.10 V	5.0	22.6	12	68
Graphite (Proc. 3)	1 s −0.15 V/6 s 0.10 V	4.1	20.5	14	49
PANI (Proc. 3)	1 s −0.15 V/30 s 0.10 V	12.1	14.5	19	36
POAP (Proc. 3)	1 s −0.15 V/30 s 0.10 V	23.5	14.7	19	36

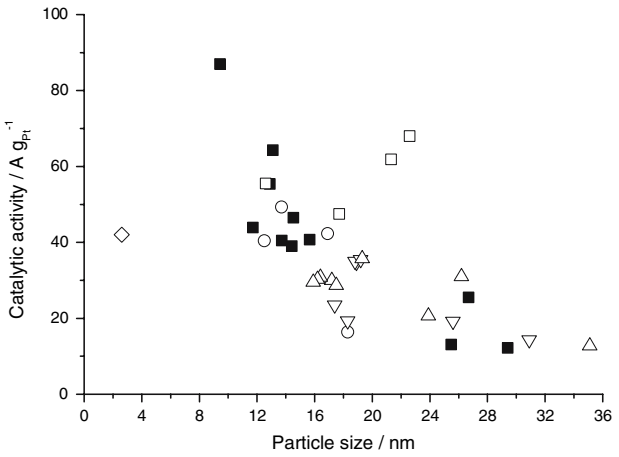

Fig. 8 Relationship between particle size and catalytic activity in methanol oxidation on (◇) Pt/Vulcan (Ref. [37], (■) Pt/macroporous carbon, (○) Pt/graphite and (□) Pt/glassy carbon electrodes, and (Δ) Pt/PANI and (▽) Pt/POAP

The particle size of deposited platinum is adjustable by a selection of the experimental conditions involved in the potential step deposition (PSD) process. The adjustable parameters are: the number of potential steps, the time of each step and the potential employed (both initial and final potentials). The average size of the platinum particles produced varied between 9 and 30 nm. The PSD process that involved multiple pulses was found to be the most suitable method in order to obtain small and uniform platinum particles (regardless of the support used). The electrocatalytic activity of Pt/carbon electrodes was investigated, in a 0.1 M CH_3OH + 0.5 M H_2SO_4 solution, by cyclic voltammetry (from 0.06 to 1.0 V with a scan rate of 10 mV s^{-1}). The high catalytic activity of the macroporous carbon (with respect to the other carbon electrodes) is thought to be a result of the 3D character of this support. It was found that the structure of the carbon support has a strong influence on the nature of the platinum particles deposited, which in turn affects the catalytic activity.

Acknowledgements The authors thank Spanish *Ministerio de Educación y Ciencia* (Projects CTQ2006-08958/PPQ and MAT2004-1479) and the EU (FEDER) for financial support.

References

1. Lordi V, Yao N, Wei J (2001) Chem Mater 13:733
2. Endo M, Kim YA, Ezaka M, Osada K, Yanagiswa T, Hayashi T, Terrones M, Dresselhaus MS (2003) Nano Lett 3:723
3. Boxall DL, Deluga GA, Kenik EA, King WD, Lukehart CM (2001) Chem Mater 13:891
4. Solla-Gullón J, Montiel V, Aldaz A, Clavilier J (2000) J Electroanal Chem 491:69
5. Liu ZL, Lee JY, Han M, Chen WX, Gan LM (2002) J Mater Chem 12:2453
6. Li WZ, Liang CH, Zhou WJ, Qiu JS, Zhou ZH, Sun GQ, Xin Q (2003) J Phys Chem 107:6292
7. Yu G, Chen W, Zhao J, Nie Q (2006) J Appl Electrochem 36:1021
8. Chen WX, Zhao J, Lee JY, Liu ZL (2005) Mater Chem Phys 91:124
9. Xue XH, Lu TH, Liu CP, Xing W (2005) Chem Commun 12:1601
10. He P, Liu H, Li Z, Li J (2005) J Electrochem Soc 152:E146
11. Tang H, Chen J, Nie L, Liu D, Deng W, Kuang Y, Yao S (2004) J Colloid Interface Sci 269:26
12. Plyasova LM, Molina IY, Gavrilov AN, Cherepanova SV, Cherstiouk OV, Rudina NA, Savinova ER, Tsirlina GA (2006) Electrochim Acta 51:4477
13. Ye J, Cui H, Wen Y, Zhang W, Xu G, Sheu F (2006) Microchim Acta 152:267
14. Tang H, Chen J, Yao S, Nie L, Kuang Y, Huang Z, Wang D, Ren Z (2005) Mater Chem Phys 92:548
15. He Z, Chen J, Liu D, Tang H, Deng W, Kuang Y (2004) Mater Chem Phys 85:396
16. Duarte MME, Pilla AS, Sieben JM, Mayer CE (2006) Electrochem Commun 8:159
17. Ueda M, Dietz H, Anders A, Kneppe H, Meixner A, Plieth W (2002) Electrochim Acta 48:377
18. Zoval JV, Lee J, Gorer S, Penner RM (1998) J Phys Chem B 102:1166
19. Burchell TD (1999) In: Carbon materials for advances technologies. Pergamon, New York
20. Marsh H, Rodriguez-Reinoso F (1997) In: Sciences of carbon materials. Publicaciones de la Universidad de Alicante, Alicante
21. Kinoshita K (1998) In: Carbon, electrochemical and physicochemical properties. Wiley, New York
22. Montilla F, Morallón E, Vázquez JL, Alcañiz-Monge J, Cazorla-Amorós D, Linares-Solano A (2002) Carbon 40:2193
23. Berenguer-Murcia A, Morallón E, Cazorla-Amorós D, Linares-Solano A (2005) Micropor Mesopor Mater 78:159
24. Montilla F, Morallón E, Duo I, Comninellis C, Vázquez JL (2003) Electrochim Acta 48:3891
25. Malinauskas A (1999) Synth Met 107:75
26. Podlovchenko BI, Andreev VN (2002) Russ Chem Rev 71:837
27. Arias-Pardilla J (2007) PhD Thesis, University of Alicante
28. Paunovic M, Schlesinger M (1998) In: Fundamentals of electrochemical deposition. Wiley Interscience, New York
29. Scharifker B, Hills G (1983) Electrochim Acta 28:879
30. Bade K, Tsakova V, Schultze JW (1992) Electrochim Acta 37:2255
31. Gloaguen F, Léger JM, Lamy C, Marmann A, Stimming U, Vogel R (1999) Electrochim Acta 44:1805
32. Hernández N, Ortega JM, Coi M, Ortiz R (2001) J Electroanal Chem 515:123
33. Tang YW, Zhang LL, Wang YN, Zhou YM, Gao Y, Liu CP, Xing W, Lu TH (2006) J Power Sources 162:124
34. Gènies L, Faure R, Durand R (1998) Electrochim Acta 44:1317
35. Kim SS, Nah YC, Noh YY, Jo J, Kim DY (2006) Electrochim Acta 51:3814
36. Wang HJ, Yu H, Peng F, Lv P (2006) Electrochem Commun 8:499
37. Sevilla M, Sanchís C, Valdés-Solís T, Morallón E, Fuertes AB (2007) J Phys Chem C 111:9749
38. Frelink T, Visscher W, van Veen JAR (1995) J Electroanal Chem 382:65
39. Bergamaski K, Pinheiro ALN, Teixeira-Neto E, Nart FC (2006) J Phys Chem B 110:19271